Circular TE_{0n} Mode Filters for Guided Millimeter-Wave Transmission

KUNIO HASHIMOTO

Abstract—A millimeter-wave circular TE_{01} mode waveguide generates undesired circularly symmetric modes (TE_{02}, TE_{03} modes, etc.) in bends or at discontinuities along a waveguide line. This paper describes the theory and experiment on the TE_{02} and TE_{03} mode filters developed for guided millimeter-wave transmission.

The experimental results of two improved TE_{03} mode filters show that the attenuation of the TE_{03} mode is more than 16 dB for one type over the 40–70-GHz range. The TE_{01}-mode insertion loss of another type is about 0.2 dB over the 40–80-GHz range.

The present mode filters can be applied to various high-speed guided millimeter-wave systems currently under development.

I. INTRODUCTION

IN the guided millimeter-wave communication systems [1], [2], the diameter of a circular TE_{01} mode waveguide is chosen to be much greater than a free-space wavelength in order to reduce the transmission loss. However, a large number of higher modes are generated at bends or at discontinuities along the waveguide. In particular, circularly symmetric modes (TE_{02}, TE_{03} modes, etc.) are generated at circular waveguide corners (the so-called miter elbow [3], capable of sharply bending waveguides) and at half-mirrors for use in the Michelson-interferometer-type band-splitting filters [4]; helix waveguides are inefficient for absorbing these modes. Therefore, the development of the TE_{0n} mode filters is important for improvement of the transmission characteristics.

Several mode filters have been proposed [5]–[8]. However, none of the proposed filters seem practical because of their limited inner diameters.

This paper describes new TE_{0n} mode filters having the same diameter as that of the waveguide line.

II. STRUCTURE AND OPERATING PRINCIPLE

Overall layout of the prototype TE_{02} mode filter [9] is shown in Fig. 1. The TE_{03} mode filter is similar to the TE_{02} mode filter, except for the absence of a semicircular dielectric. A circular waveguide with radius R is divided into two semicircular waveguides by a metallic sheet. One of the waveguides has a smaller radius R' and is connected to the tapered semicircular waveguides (tapering from R to R'). Resistive sheets are connected to the metallic sheet. In addition, the TE_{02} mode filter has a semicircular dielectric with dielectric constant ϵ_r and thickness t,

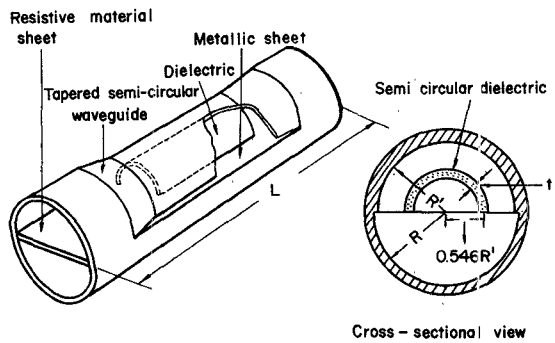

Fig. 1. Structure of the prototype TE_{02} mode filter. The prototype TE_{03} mode filter is similar to the TE_{02} mode filter except for the absence of a semicircular dielectric.

disposed at the position of $0.546R'$, where the electric field of the TE_{02} mode is zero.

The filter is designed in such a manner that two semicircular guides produce the opposite phase difference for the undesired modes and zero difference for the signal mode. The undesired TE_{0n} modes are thus destructively combined at the output of semicircular guides and converted into the unsymmetric modes (mainly, TE_{1n}, TE_{3n}, TM_{1n} modes, etc.). The Appendix shows the formulation of these modes. The electric field of these modes is parallel to the resistive sheet, resulting in high attenuation. On the other hand, the semicircular TE_{01} modes are converted into the circular TE_{01} mode. Because the electric field of this mode is perpendicular to the resistive sheet, the conversion loss is very small. A mode filter having an analogous principle has been reported [10]. The difficulty of the reported filter is due to higher insertion loss because of nonzero phase difference between two semicircular TE_{01} modes.

The phase difference is produced by: 1) decreasing or increasing one of guide radii, 2) inserting a dielectric in one of the guides, and 3) introducing the inductive or capacitive susceptances. To accomplish broad-band characteristics, e.g., the 43–87-GHz range [1], the phase difference must be chosen close to 180° for the undesired modes and zero for the signal mode. This is possible by suitably combining the aforementioned methods.

III. DESIGN AND EXPERIMENTAL RESULTS OF THE PROTOTYPE TE_{02} AND TE_{03} MODE FILTERS

The phase difference is determined by the difference of the phase constant of two semicircular waveguides. If the low-density dielectric is used, the perturbation method

Manuscript received March 20, 1975; revised July 7, 1975.
The author is with the Yokosuka Electrical Communication Laboratory, Nippon Telegraph and Telephone Public Corporation, Yokosuka-shi, Tokyo, Japan.

[11] is sufficient for calculating this phase difference. The results are given by

$$\Delta\theta_{[0n]}{}^{(1)} \simeq \pi\lambda \frac{x_{[0n]}{}^2}{2\pi^2} \frac{R - R'}{R \cdot R'^2} \cdot l_{eq} \tag{1}$$

$$\Delta\theta_{[0n]}{}^{(2)} \simeq \pi \cdot 2(\epsilon_r - 1) \frac{\lambda_{g[0n]}}{\lambda^2} \frac{t \cdot r_1}{R^2} \left(\frac{J_0'(x_{[0n]} r_1/R)}{J_0(x_{[0n]})} \right)^2 \cdot h \tag{2}$$

where

l_{eq} equivalent length of the semicircular section having radius R' (including the tapered section);
$x_{[0n]}$ the nth root of $J_1(x) = 0$;
$\lambda_{g[0n]}$ guide wavelength of the TE_{0n} mode;
t, r_1, h thickness, radius, and length of the semicircular dielectric, respectively.

The attenuation of the TE_{0n} mode is given by

$$A_{[0n]} = 10 \log_{10} \{\cos(\Delta\theta_{[0n]}/2)\}^2 \quad \text{(dB)}. \tag{3}$$

In general, the tapered semicircular waveguides generate the TE_{0n} ($n \geq 2$) modes. Therefore, length of the tapered section and radius difference must be chosen to be as long as and as small as possible. However, it is found possible to cancel the TE_{0n} modes generated at two tapered sections by adjusting the length in between. The generated TE_{0n} modes theoretically can be suppressed to be less than -40 dB for the 40–80-GHz range.

Table I shows the design parameters of the TE_{02} mode filter. A foamed polystyrene ($\epsilon_r = 1.03$) is inserted into one of the semicircular guides. The frequency is chosen to be 50 GHz, where the maximum attenuation for the TE_{02} mode and the lowest loss for the TE_{01} mode result.

Fig. 2 compares the theoretical and experimental results. The experimental value is in good agreement with the theoretical one. The insertion loss is less than 0.8 dB over the 40–80-GHz range. The theoretical value includes the loss due to the phase difference of the TE_{01} mode, the mode conversion loss in the tapered sections (0.09 dB), the heat loss in the wall (0.09 dB), and the loss due to tan δ of the dielectric (0.04 dB). Fig. 2 shows that the attenuation of the TE_{02} mode is more than 6 dB over the 40–80-GHz range and the influence of the dielectric is almost negligible for the TE_{02} mode.

TABLE I
DESIGN PARAMETERS OF PROTOTYPE TE_{02} MODE FILTER

Overall filter length	650 mm
Length of smaller semi-circular guide	300 mm
Tapered waveguide length	75 mm
Filter radius	25.5 mm
Radius of smaller semi-circular guide	23.0 mm
Resistive sheet length	100 mm
Dielectric thickness	2.0 mm
Dielectric constant	1.03
Dielectric length	90 mm

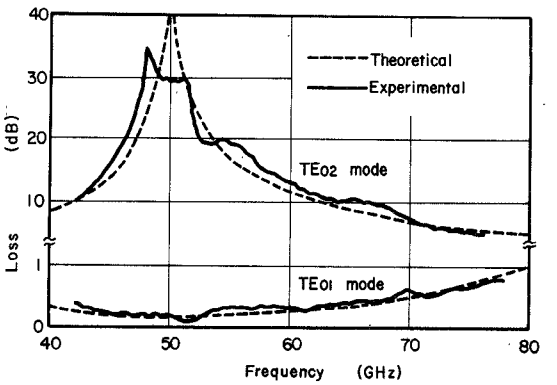

Fig. 2. Frequency response of prototype TE_{02} mode filter.

TABLE II
DESIGN PARAMETERS OF PROTOTYPE TE_{03} MODE FILTER

Overall filter length	598 mm
Length of smaller semi-circular guide	198 mm
Tapered waveguide length	100 mm
Filter radius	25.5 mm
Radius of smaller semi-circular guide	24.0 mm
Resistive sheet length	100 mm

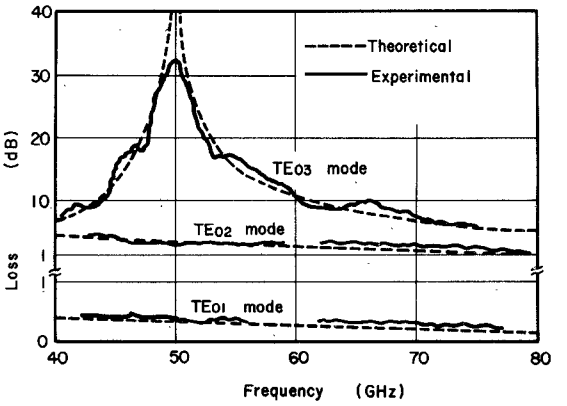

Fig. 3. Frequency response of prototype TE_{03} mode filter.

Table II shows the design parameters of the TE_{03} mode filter. The phase difference of the TE_{03} mode is chosen to be 180° at 50 GHz. The phase difference of the TE_{01} mode is so small that the TE_{03} mode filter requires no dielectric. The experimental results of the TE_{03} mode filter are shown in Fig. 3. The insertion loss of the TE_{01} mode is less than 0.4 dB and the attenuation of the TE_{03} mode is more than 6 dB over the 40–80-GHz range. This filter has an advantage of more or less absorbing the TE_{02} mode in the lower frequency range. The attenuation of the TE_{02} mode is about 4 dB in the neighborhood of 40 GHz.

It is instructive to compare this mode filter to the well-known coupled type [6]. In the coupled-mode filter with a 50-mm inner diameter, the filter length is expected to be 2 m. This is four times longer than the one presented in this paper. The fabrication accuracy of the coupled type

is stringent. For example, the maximum attenuation of the undesired mode is reduced to be 10 dB for a 0.2-mm fabrication error. In this mode filter, the frequency giving infinite loss is shifted only 2 GHz for the same error without reducing the maximum attenuation.

IV. DESIGN AND EXPERIMENTAL RESULTS OF TWO IMPROVED TE_{0n} MODE FILTERS

A large number of mode filters are required for the "cable-tunnel" millimeter-wave system [12]. For such applications more ambitious mode filters must be developed in which the TE_{01} mode insertion loss is extremely low, yet keeping high attenuation for the undesired modes over a broad frequency range. This section describes the design and experimental results of two improved TE_{0n} mode filters. They are named as high-attenuation type and low-insertion type.

A. High-Attenuation-Type TE_{0n} *Mode Filters*

In the prototype mode filters, the phase difference is produced by decreasing the guide radius. Equation (1) shows that the phase difference is inversely proportional to the frequency. On the other hand, (2) shows that the phase difference caused by the dielectric is proportional to the frequency. Hence by combining these two effects, it is possible to produce 180° phase difference for the undesired modes over the broad frequency range. Applying this principle to the mode filter results in the high-attenuation-type mode filter.

A cross-sectional view of the TE_{02} and TE_{03} mode filters is shown in Fig. 4. An additional dielectric is mounted at the wall of one of the semicircular guides. The dielectrics inserted in these filters are foamed polystyrene ($\epsilon_r = 1.03$) and polyethylene ($\epsilon_r = 2.3$), respectively. The phase difference due to the foamed polystyrene is again calculated from (2) and depicted in Fig. 5. The phase difference due to the polyethylene can be calculated from the continuity of the electromagnetic field at the interface between the dielectric and space. The phase constant of the semicircular TE_{0n} modes is determined by the following characteristic equation:

$$\frac{1}{h}\frac{J_0(hR_1)}{J_0'(hR_1)} = \frac{1}{l}\frac{J_0(lR_1)N_0'(lR_2) - N_0(lR_1)J_0'(lR_2)}{J_0'(lR_1)N_0'(lR_2) - N_0'(lR_1)J_0'(lR_2)} \quad (4)$$

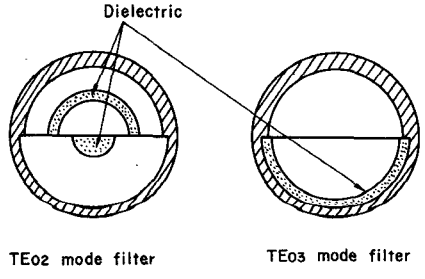

Fig. 4. Cross-sectional views of high-attenuation-type TE_{0n} mode filters. The dielectrics inserted in the TE_{02} and TE_{03} mode filters are foamed polystyrene ($\epsilon_r = 1.03$) and polyethylene ($\epsilon_r = 2.3$), respectively.

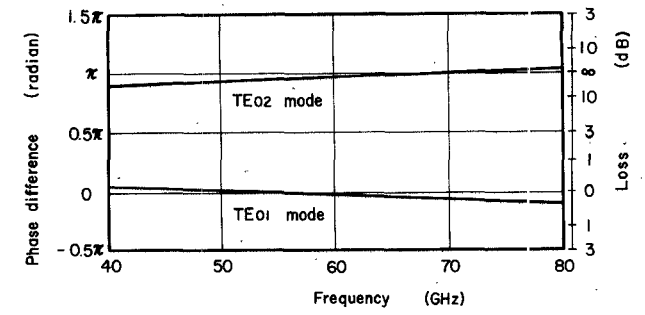

Fig. 5. Phase difference for high-attenuation-type TE_{02} mode filter. Relation between the phase difference and the attenuation is shown in (3).

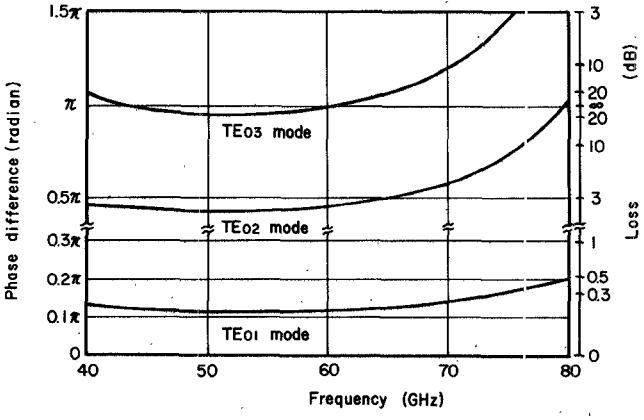

Fig. 6. Phase difference for high-attenuation-type TE_{03} mode filter.

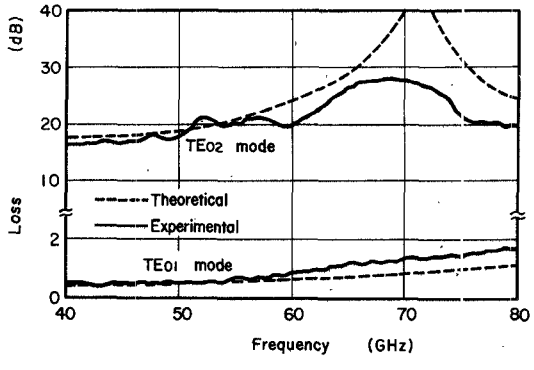

Fig. 7. Frequency response of high-attenuation-type TE_{02} mode filter.

$$h^2 - k_0^2 = l^2 - \epsilon_r k_0^2 \quad (5)$$

where

- h,l transverse wavenumber in space and dielectric, respectively;
- R_1,R_2 inner and outer radii of the semicircular dielectric, respectively.

Fig. 6 shows the phase difference for the TE_{0n} ($n = 1,2,3$) modes.

Figs. 7 and 8 show the experimental results of the TE_{02} and TE_{03} mode filters along with the theoretical one. The attenuation of the TE_{02} mode is more than 17 dB for the 40–80-GHz range. The attenuation of the TE_{03} mode is

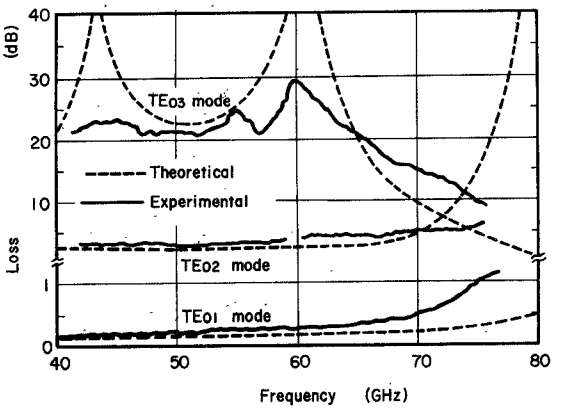

Fig. 8. Frequency response of high-attenuation-type TE_{03} mode filter.

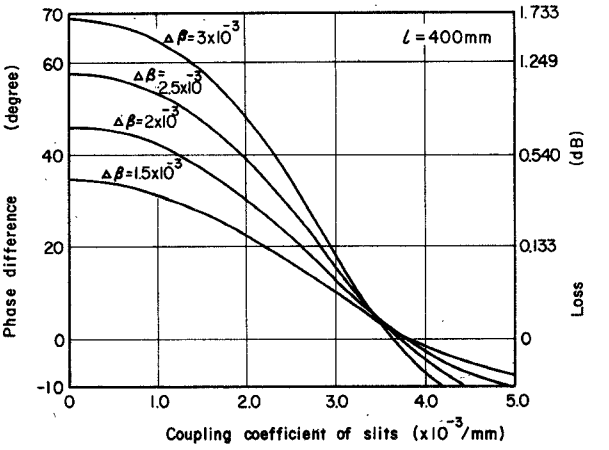

Fig. 9. Phase difference versus amplitude coupling coefficient of slits. Coupling length is 400 mm.

more than 16 dB. The insertion loss of the TE_{01} mode is less than 0.5 dB for the same frequency range.

B. Low-Insertion-Type TE_{0n} Mode Filters

The insertion loss of prototype TE_{0n} mode filters is mainly due to the phase difference of the TE_{01} mode. Therefore, for reducing the insertion loss, it is necessary to decrease the phase difference. Insertion of the dielectric can reduce the phase difference of the TE_{01} mode. However, this method is less effective because of the difficult support of the semicircular dielectric and of the loss increase due to tan δ of the dielectric. To overcome this difficulty, the coupling slits at the common wall of the semicircular waveguides can be used in place of the dielectric.

The coupling between the two waveguides having different phase constant can reduce the phase difference of the two guides. Phase difference $\Delta\theta$ due to the coupling slits is given by the following equation:

$$\begin{cases} \Delta\theta = \left| \tan^{-1} \dfrac{(\varphi - 2C)\sin\Delta}{\Gamma\cos\Delta} + \tan^{-1} \dfrac{(\varphi + 2C)\sin\Delta}{\Gamma\cos\Delta} \right| \\ \varphi = (\beta_1 + C_{11}) - (\beta_2 + C_{22}) \\ \Gamma = (\varphi^2 + 4C^2)^{1/2} \\ \Delta = \Gamma \cdot l/2 \end{cases} \tag{6}$$

where

β_1, β_2 phase constant of two semicircular guides;
C_{11}, C_{22} reaction of coupling slit in coupled guides;
C amplitude coupling coefficient of slit per unit length;
l length of the semicircular guide.

Fig. 9 shows the phase difference versus coupling coefficient of slits. The coupling coefficient of 5×10^{-3}/mm is small enough to design the practical coupling slits, and thus it is possible to make the phase difference fairly small, resulting in low insertion loss.

Fig. 10 shows the structure of the TE_{02} and TE_{03} mode filters whose slits are arranged at the flat metal wall

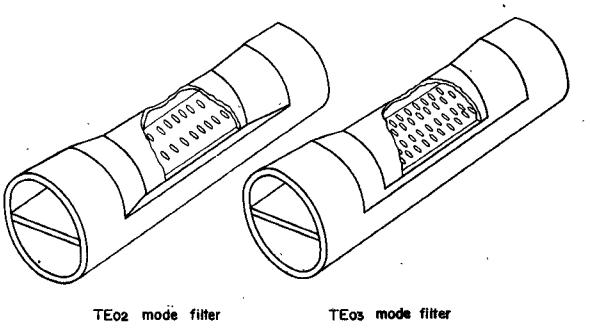

Fig. 10. Structure of low-insertion-loss-type TE_{0n} mode filters arranged two and four row slits at the flat metal wall.

along the axial direction. These mode filters must be designed to couple the TE_{01} modes and to decouple the undesired modes. In an overmoded waveguide having a large diameter, the coupling is larger for the transverse magnetic field H_r than for the longitudinal magnetic field H_z. The slits are thus opened at the position where the H_r of the undesired TE_{0n} modes are zero. The low-insertion-type mode filters have almost the same dimensions as the prototypes, except for slits on the flat metal wall. The design parameters of the coupling slits are tabulated in Table III.

Experimental results of the TE_{02} mode filters are shown in Fig. 11, in comparison with those of the prototype TE_{02} mode filter. The insertion loss of the TE_{01} mode is less than 0.7 dB over the 40–80 GHz. Experimental results of the TE_{03} mode filter are shown in Fig. 12. The insertion loss of the TE_{01} mode is as small as 0.2 dB over the same frequency range. It is noted that the attenuation of the undesired modes is unchanged. Frequency shift due to coupling slits is about 1 GHz and coupling slits do not yield additional undesired modes.

V. CONCLUSION

The TE_{0n} mode filters can improve the transmission characteristics of various guided millimeter-wave transmission systems. This paper has presented the theory and experiment on the new types of the TE_{0n} mode filters.

TABLE III
DESIGN PARAMETERS OF COUPLING SLITS

Low Insertion Loss Type Mode Filter	Slit Length	Slit Width	Distance Between Adjacent Slits	Number of Slits per Row	Slit Postion
TE_{02} mode filter (two row slits)	2.5 mm	1.2 mm	1.5 mm	237	13.5 mm
TE_{03} mode filter (four row slits)	2.4 mm	1.2 mm	1.5 mm	253	9.6 mm 17.6 mm

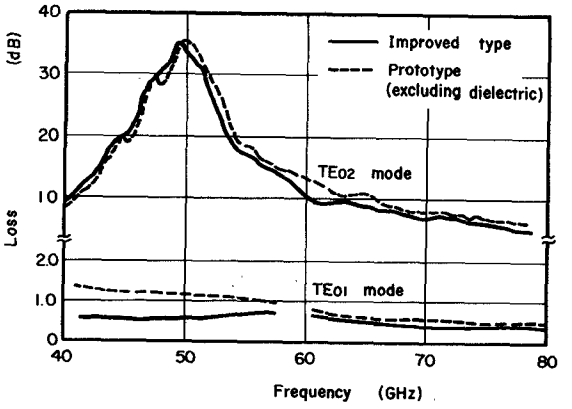

Fig. 11. Frequency response of low-insertion-loss-type TE_{02} mode filter.

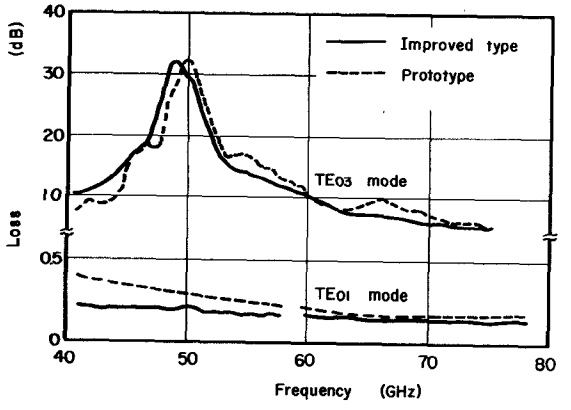

Fig. 12. Frequency response of low-insertion-loss-type TE_{03} mode filter.

They all have a 51-mm inner diameter, capable of being directly connected to the waveguide line.

In addition to the prototypes of the TE_{02} and TE_{03} mode filters, the more ambitious types have been developed. They are categorized as high-attenuation types and low-insertion types. The former TE_{03} mode filter has an additional semicircular dielectric on the flat wall, resulting in more than 16-dB attenuation over the 40–70-GHz range. In this case, the insertion loss is less than 0.5 dB in the same frequency range. The latter is constructed by opening coupling slits at the common wall. The insertion loss is less than 0.7 dB for the TE_{02} mode filter and 0.2 dB for the TE_{03} mode filter.

The mode filters presented here should open new applications in various guided millimeter-wave systems currently under development.

APPENDIX

MODE CONVERSIONS CAUSED AT A TRANSITION FROM DUAL SEMICIRCULAR TO CIRCULAR WAVEGUIDES

Semicircular TE_{0n} modes having mutually opposite phase create a magnetic wall at a transition shown in Fig. 13. The amplitudes of the converted and reflected modes are derived from the boundary conditions and mode orthogonality.

The boundary conditions are written as follows:

$$V_{[0n]}\boldsymbol{e}_{[0n]}{}^{(i)} + RV_{[0n]}\boldsymbol{e}_{[0n]}{}^{(i)} + \sum_{mn}{}' V_{mn}\boldsymbol{e}_{mn}{}^{(i)} = \sum_{pq} U_{pq}\boldsymbol{e}_{pq}{}^{(t)} \quad (7)$$

$$V_{[0n]}\boldsymbol{h}_{[0n]}{}^{(i)} - RV_{[0n]}\boldsymbol{h}_{[0n]}{}^{(i)} - \sum_{mn}{}' \gamma_{mn}V_{mn}\boldsymbol{h}_{mn}{}^{(i)} = \sum_{pq} \gamma_{pq}U_{pq}\boldsymbol{h}_{pq}{}^{(t)} \quad (8)$$

where

$V_{[0n]}, RV_{[0n]}$ amplitude of the incident and reflected TE_{0n} modes, respectively;

V_{mn}, U_{pq} amplitude of the reflected and transmitted modes;

$\boldsymbol{e}^{(i)}, \boldsymbol{e}^{(t)}$ mode function of electric field for the incident and transmitted modes, respectively;

$\boldsymbol{h}^{(i)}, \boldsymbol{h}^{(t)}$ mode function of magnetic field for the incident and transmitted modes;

γ_{mn} $Y_{mn}/Y_{[0n]}$;

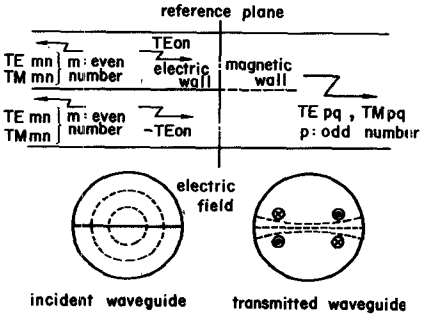

Fig. 13. Mode conversion at the junction between two semicircular and circular waveguides due to the opposite-phase TE_{0n} mode excitation.

$\sum'_{mn}$ mode sum, except for the incident TE_{0n} mode.

Multiplying (7) and (8) by mode function and integrating over the cross section of a semicircular guide result in the following equations:

$$(1 + R)V_{[0n]} = \sum_{pq} U_{pq}\Phi_{pq[0n]} \tag{9}$$

$$V_{mn} = \sum_{pq} U_{pq}\Phi_{pqmn} \tag{10}$$

$$(1 + R)V_{[0n]}\Phi_{[0n]pq} + \sum'_{mn} V_{mn}\Phi_{mnpq} = U_{pq} \tag{11}$$

$$(L - R)V_{[0n]} = \sum_{pq} U_{pq}\psi_{pq[0n]} \tag{12}$$

$$-\gamma_{mn}V_{mn} = \sum_{pq} \gamma_{pq}U_{pq}\psi_{pqmn} \tag{13}$$

$$(1 - R)V_{[0n]}\psi_{[0n]pq} - \sum'_{mn} \gamma_{mn}V_{mn}\psi_{mnpq} = \gamma_{pq}U_{pq} \tag{14}$$

where

$$\Phi_{pqmn} = \int_0^{\pi}\int_0^{R} \boldsymbol{e}_{pq}^{(t)} \cdot \boldsymbol{e}_{mn}^{(i)} r \cdot dr\, d\varphi$$

$$\psi_{pqmn} = \int_0^{\pi}\int_0^{R} \boldsymbol{h}_{pq}^{(t)} \cdot \boldsymbol{h}_{mn}^{(i)} r \cdot dr\, d\varphi.$$

If $V_{mn} = 0$, the zero-order amplitude of the transmitted wave U_{pq} is derived from (11) and (12) as follows:

$$U_{pq}^{0} = \frac{2}{1 + \gamma_{pq}} \cdot V_{[0n]}\Phi_{[0n]pq}. \tag{15}$$

The first-order amplitude of the reflected waves is then derived from (10) and (15), as follows:

$$V_{mn}^{1} = \sum_{pq} U_{pq}^{0}\Phi_{pqmn}. \tag{16}$$

Using (11), (14), and (16), amplitude of the transmitted waves in the first-order approximation is derived to be

$$U_{pq}^{1} = \frac{2}{1 + \gamma_{pq}} V_{[0n]}\Phi_{[0n]pq} + \frac{2}{1 + \gamma_{pq}} \sum'_{mn} (1 - \gamma_{mn})V_{mn}^{1}\Phi_{mnpq}. \tag{17}$$

By iterating the preceding operation, a highly accurate solution can be derived. Mode filters described in this paper have a large inner diameter and thus the incident semicircular TE_{0n} modes are converted mainly into the transmitted circular modes. Namely, it can be assumed that V_{mn} is nearly equal to zero. Therefore, first-order approximation is sufficient for calculation of amplitude of the reflected and transmitted modes.

The reflection coefficient is derived from (9) and (12) as follows:

$$\frac{1 - R}{1 + R} = \frac{\sum \gamma_{pq}U_{pq}\Phi_{pq[0n]}}{\sum U_{pq}\Phi_{pq[0n]}}. \tag{18}$$

TABLE IV
AMPLITUDE OF TRANSMITTED MODES FOR INCIDENT TE_{02} MODES (AT 50 GHz, 51 MM)

TE mode	Amplitude	TM mode	Amplitude
TE_{11}	j0.12810	TM_{11}	-j0.18746
TE_{12}	-j0.47936	TM_{12}	j0.33696
TE_{13}	-j0.60320	TM_{13}	-j0.10712
TE_{31}	j0.10818	TM_{31}	-j0.14532
TE_{32}	-j0.08944	TM_{32}	j0.20308
TE_{51}	j0.10056	TM_{51}	-j0.12832

TABLE V
AMPLITUDE OF TRANSMITTED MODES FOR INCIDENT TE_{03} MODES (AT 50 GHz, 51 MM)

TE mode	Amplitude	TM mode	Amplitude
TE_{12}	j0.14500	TM_{12}	-j0.15534
TE_{13}	-j0.49764	TM_{13}	j0.26640
TE_{14}	-j0.61164	TM_{14}	-j0.10158
TE_{31}	j0.06290	TM_{31}	-j0.04370
TE_{32}	j0.14104	TM_{32}	-j0.10812
TE_{51}	j0.07672	TM_{51}	-j0.07868

TABLE VI
REFLECTION COEFFICIENTS (AT 50 GHz, 51 MM)

Incident mode	Coefficient
TE_{01}	0.00343
TE_{02}	0.00449
TE_{03}	0.00136

Tables IV and V show the amplitudes of the transmitted modes for the incident TE_{02} and TE_{03} modes, respectively. Table VI shows reflection coefficients for incident TE_{0n} (n = 1,2,3) modes. These analytical results show that the transmitted modes are only the TE_{mn} and TM_{mn} modes having an odd number of m and that the reflected waves are less than −47 dB.

ACKNOWLEDGMENT

The author wishes to thank Dr. S. Shimada and Dr. K. Koyama for their suggestions and remarks concerning the research presented in this paper.

REFERENCES

[1] S. Seki *et al.*, "Transmitter-receivers for the millimeter-wave transmission system in the 43–87 GHz range," in *Proc. 1974 4th European Microwave Conf.* (Sept. 1974), p. 624, Paper C-9.
[2] T. A. Abele *et al.*, "A high-capacity digital communication system using TE_{01} transmission in circular waveguide," *IEEE Trans. Microwave Theory Tech. (Special Issue on Microwave Communications)*, vol. MTT-23, pp. 326–333, Apr. 1975.
[3] E. A. J. Marcatili, "Miter elbow for circular electric mode," in *Proc. Symp. Quasi-Optics.* New York: Polytechnic, 1964, p. 535.
[4] N. Suzuki, "A 40–120-GHz Michelson interferometer-type band-splitting filter," *IEEE Trans. Microwave Theory Tech.* (Short Papers), vol. MTT-22, pp. 565–566, May 1974.
[5] N. Kumagai *et al.*, "TE_{0n} mode filters for TE_{01} mode wave-

guide," *J. Inst. Elec. Commun. Eng. Jap.*, vol. 47, Mar. 1964.
[6] Von S. Seldmair, "Ein breitbandiges Dämpfungsglied zur gleichzeitigen Bedämpfung Höherer H_{0n}-Wellen in H_{01}-Übertragung-sleitungen," *Frequenz*, vol. 22, p. 118, 1968.
[7] S. Shimada, "TE_{02} mode filter for TE_{01} mode circular waveguide at millimeter wavelengths," *Rev. Elec. Commun. Lab.*, vol. 16, Jan.–Feb. 1968.
[8] K. Hashimoto *et al.*, "Wave coupled TE_{02} mode filters," *Rev. Elec. Commun. Lab.*, vol. 22, Jan.–Feb. 1974.
[9] K. Hashimoto *et al.*, "Circular TE_{0n} mode filters for a guided millimeter-wave transmission," in *1973 G-MTT Int. Microwave Symp. Dig.*, pp. 19–21, 1973.
[10] M. V. Persikov, "Brief communication filter for the H_{02}-wave in a circular waveguide," *Radio-teknika Electron.*, vol. 6, p. 444, 1961.
[11] J. L. Altman, *Microwave Circuits*. New York: Van Nostrand, 1964.
[12] K. Kondoh *et al.*, "Analysis of transmission characteristics of circular waveguide installed in cable tunnels," *Rev. Elec. Commun. Lab.*, vol. 19, Nov.–Dec. 1971.

Wide-Band Varactor-Tuned Coaxial Oscillators

COLIN D. CORBEY, ROBERT DAVIES, AND ROBERT A. GOUGH

Abstract—**An experimental investigation into the effects of package and circuit reactances on wide-band varactor-tuned oscillators is described. The results are used to design an *X*-band Gunn coaxial oscillator with a tuning range in excess of 3 GHz. It is shown that the stray reactances, junction capacitance, and bond-wire inductance affect the varactor tuning characteristics. The characteristics are conveniently displayed by the reflection phase variation with tuning voltage and frequency. A general theory for wide-band varactor-tuned oscillators is presented which is related to the impedance characteristics. These results are used to design three coaxial varactor-tuned oscillators. The first two oscillators are series arrangements while the third oscillator is a parallel arrangement. A simple circuit technique is used to improve the tuning range of each arrangement. This technique is shown to increase the coupling to the varactor diode and decrease the oscillator *Q* by reactance compensation.**

I. INTRODUCTION

WHILE considerable microwave-circuit design information exists for varactor-tuned oscillators, little has been done to optimize the wide-band operation. The more successful wide-band oscillators use varactor diodes either in miniature packages [1], [2] or unencapsulated in microwave integrated circuits [3]. In the present investigation, attempts are made to obtain wide-band operation at *X* band using the standard S4 [4] package by appropriate choice of circuit impedance, varactor-diode parameters, including bond-wire inductance, and diode mounting arrangements. Other authors [5] have studied the importance of package parasitics in the design of transferred-electron amplifiers and were able to optimize the package for *X*–*Ku*-band applications.

The design feature of wide-band varactor-tuned oscillators is that the varactor junction capacitance should be the dominant resonating reactance. Although the resonant frequencies of the S4 package are lower than those of the miniature package, large tuning ranges at *X* band have been reported in a coaxial arrangement (1.1 GHz) [6], a full-height waveguide structure (over 1 GHz) [7], and a reduced-height waveguide structure (1.95 GHz) [8]. In this work, coaxial circuits are investigated because of their low *Q* and ease of characterization.

Microwave-diode impedance measurements are shown to substantially agree with calculated values using the equivalent-circuit models developed elsewhere [9]–[11]. A general theory of wide-band varactor-tuned oscillators is presented and the importance of the varactor impedance–voltage relationship as displayed on a Smith chart by the varactor reflection phase variation is discussed. The concept of tuning phase is introduced. The tuning phase is shown to be related to the oscillator tuning range and is dependent on the frequency, circuit stray reactances, bond-wire inductance, and varactor junction capacitance.

Three coaxial varactor-tuned *X*-band Gunn or IMPATT oscillators are finally described; the first two arrangements incorporate the varactor and active devices in series; the third incorporates the devices in parallel. A varactor diode with a large tuning phase is used to realize a varactor tuning range in excess of 3 GHz with a Gunn device.

II. MICROWAVE-DIODE IMPEDANCE CHARACTERISTICS

Package and circuit parasitic reactances associated with the S4 package in series and shunt-mounted coaxial arrangements have been reported elsewhere [9]–[11], yield-

Manuscript received June 18, 1974; revised May 17, 1975. The work of one of the authors (R.A.G.) was supported by a United Kingdom Science Research Council Grant.

C. D. Corbey and R. Davies are with the Mullard Research Laboratories, Redhill, Surrey, England.

R. A. Gough was with the University of Bradford, Bradford, Yorks., England. He is now with ESTEC, Domeinweg, Noordwijk, The Netherlands.